Retrofitting Existing Combined Cycle Power Plants to Enable Carbon Circularity through Power-to-Methane Energy Storage

Diego Santamaría, Alberto Almena, Antonio Sánchez, Mariano Martín*

Department of Chemical Engineering, University of Salamanca, Plz Caídos 1-5, Salamanca, 37008, SPAIN.

Abstract

Energy storage is a critical component in the transition to a renewable based energy system. To face this challenge, Power-to-X technologies are gaining increased attention. This study investigates the conversion of surplus electricity from wind and solar sources into hydrogen, and subsequently into methane, utilizing existing natural gas infrastructure for efficient storage, transport and conversion into electricity. The process consists of two main stages: first, the production of methane using Power-to-X technologies during periods of excess renewable energy production. Second, the generation of electricity during peak demand, with CO_2 captured for reuse in methane synthesis creating a closed carbon loop. This integrated system repurposes combined cycle power plants, developing a Power-to-Methane-to-Power (PtMtP) configuration. Two alternative combustion approaches are evaluated: oxy-combustion (OC), which simplifies CO_2 purification and air combustion or ordinary combustion or conventional combustion (CC), which requires more complex purification methods such as amine absorption or pressure swing adsorption (PSA). Results indicate that CC with CO_2 capture via amine absorption is the most profitable process, especially when it is assumed that the oxygen produced by the electrolyzer is sold. For a 400 MW CCPP, the electricity production cost ranges from 650 to 750 $/MWh when the income from oxygen sales is neglected. However, if it is assumed that the market can absorb the full output of electrolytic oxygen, the production cost decreases to between 450 and 550 $/MWh.

Keywords: Carbon capture, Hydrogen, Methane, Combined Cycle Power Plant, Power-to-Methane.

*Corresponding author: mariano.m3@usal.es

1. INTRODUCTION

The European Union's (EU) climate change mitigation strategy is driven by the the European Climate Law, which established a legally binding 2030 target of reducing net greenhouse gas emissions by at least 55% compared to 1990 levels, while aiming to achieve climate neutrality (net-zero emissions) by 2050 [1]. Achieving these objectives is fundamentally linked to transitioning towards a low-carbon energy system with a high share of renewables. This commitment has led to a record of 24.5% of the EU's energy being produced from renewable sources in 2023 [2]. However, the need to accelerate this transition has been amplified by the current uncertain geopolitical scenario, demanding a sharp reduction in the EU energy system's high dependency on external fossil fuel resources. As a direct response, the revised Renewable Energy Directive (EU/2023/2413) has established significantly more ambitious goals. The directive mandates a binding EU-wide renewable energy target of at least 42.5% by 2030, a significant increase from the previous 32% target, with an aspiration to reach 45% [3].

This ambitious energy transition necessitates a fundamental shift in the electrical power system, specifically the progressive replacement of dispatchable, conventional power plants with fluctuating renewable energy sources, such as wind and solar. The inherent intermittency and seasonal variability of these sources pose a significant challenge to grid stability and can compromise the reliability of the entire energy system [4]. Energy Storage Systems (ESS) have been proposed to manage these fluctuations and ensure a consistent and reliable power supply. Furthermore, these storage systems are a fundamental pillar for ensuring energy independence, completely eliminating the need for non-renewable resources. ESS includes a myriad of technologies that can be categorized into electrical, electrochemical, mechanical, thermal, and chemical energy storage systems [5].

Among them, green hydrogen has emerged as a particularly promising renewable chemical energy storage medium [6]. Green hydrogen can be produced through renewable-electricity-driven electrolysis. Once generated, hydrogen can be directly stored in multiple forms such as compressed gas, a liquid, or a cryocompressed fluid. Alternatively, to ease bulk transportation, enhance safety, and potentially reduce storage costs, hydrogen can be chemically stored within auxiliary materials known as hydrogen carriers [7]. Among them there are systems such as metal hydrides, Liquid Organic Hydrogen Carriers (LOHCs),

methane, methanol or ammonia [8].-Specifically, synthetic methane can be seamlessly integrated into the extensive natural gas infrastructure deployed across the EU, which encompasses long-distance transport pipelines, compressor stations, local service lines, and Combined Cycle Power Plants (CCPP) for electricity generation. The investment costs associated with deploying new large-scale energy storage and transport infrastructure, consequently, can be significantly mitigated. Moreover, in the current context, in countries where renewable energy penetration is high, these types of plants are already serving as a support for renewable generation systems, addressing the inherent variations in these renewable systems [9].

Despite the strategic benefits of leveraging the gas infrastructure, the combustion of methane (even if it comes from renewable sources) in CCPPs remains a significant point source of carbon dioxide emissions. To mitigate this, integrating Carbon Capture (CC) technology into conventional CCPPs has been deployed as a pathway for low-carbon, fossil-based electricity generation. CO_2 capture technologies are generally categorized as pre-combustion, post-combustion, and oxy-combustion. While the three systems have been explored for integration in natural gas power plants, post-combustion capture and oxy-combustion are the two primary viable strategies for conventional CCPPs [10–12] . The operation of these systems, however, requires substantial internal energy consumption. This energy penalty is caused by the need to divert a significant share of the plant's generated thermal energy, which ultimately reduces the net electricity-generation yield while enabling the capture of most of the CO_2 from the flue gas.

Specifically, post-combustion CC represents a diverse group of technologies that may be applicable to conventional CCPPs, designed to remove CO_2 from flue gases at the relatively low partial pressure conditions following combustion. This group includes four principal methods: absorption (solvent-based), adsorption (solid sorbents), membranes, and cryogenic processing [13]. Among these options, chemical absorption of CO_2 using aqueous alkanolamine solutions, such as monoethanolamine (MEA), is a mature technology [14]. Alternatively, carbon capture systems based on physical adsorption have been widely explored, reporting carbon removal yields comparable to chemical absorption technologies when applied to combustion flue gases [15].

As an effort to potentially decrease the severe energy penalty of post-combustion capture, shifting CCPP operation to oxy-combustion has also been investigated [16]. By substituting air with pure oxygen as the

oxidant, the resulting flue gas is composed almost entirely of water and CO_2, which allows for separation via a much simpler cryogenic condensing step. However, the use of pure oxygen significantly raises the combustion temperature, necessitating precise thermal control. To prevent exceeding the material limitations of the gas turbine, the injection of recycled CO_2 and steam is required to moderate and stabilize the combustion temperature. This specific configuration is known as the semi-closed combined cycle [17].

The principal objective of integrating CC into power plants is to prevent CO_2 from being vented to the atmosphere. Two distinct strategies exist for managing this captured carbon: carbon capture and storage (CCS) and carbon capture and utilization (CCU). The former involves the permanent physical sequestration of the captured CO_2 in deep geological formations, such as saline aquifers, sedimentary basins or depleted oil and natural gas reservoirs [18]. Conversely, CCU leverages CO_2 as a raw material in the manufacturing process of multiple high-value products. These products range from chemicals –e.g., methanol [19,20], urea [21] or formic acid [22,23] and synthetic fuels [24,25] to building materials [26] and polymers [27]. Among them, Power-to-methane has received great attention, in particular, for its use as energy storage system. In this process alternative, the captured CO_2 is reacted with the renewable hydrogen in a downstream unit following the methanation pathway to produce synthetic methane [28]. Meylan et al. [29] evaluated the possibility of transforming the excess of wind electricity into synthetic methane using the methanation process focusing on material availability for this new infrastructure. In the same line, Fonder et al. [30] investigated a decentralized system using low-cost electricity that can be produced in certain areas (in the case of the study, Morocco) to produce synthetic methane as an energy vector to transport energy to areas of higher consumption (in this case Belgium).

However, only a limited number of studies have specifically investigated the complete Power-to-Methane-to-Power (PtM–PtP) cycle for application in energy storage systems. Pyo et al. [31] evaluated the introduction of hydrogen into existing natural gas power plants, including the option of methanation. In their approach, hydrogen or synthetic methane is blended with fossil natural gas and used in a conventional combined-cycle plant. While this strategy may represent a straightforward pathway to emission reductions in the short term, achieving the proposed decarbonization targets ultimately requires the deployment of new technologies and the phase-out of fossil natural gas. Moreover, the authors only consider post-combustion carbon capture based on amine scrubbing. Kezibri et al. [32] investigated the

production and utilization of synthetic methane; however, their analysis is limited to oxy-fuel combustion from a thermodynamic and process perspective, without addressing the economic aspects. Prakash et al. [33] assessed the potential for increasing the energy output of existing plants using a mixture of fossil natural gas and synthetic methane, produced via methanation of a fraction of the emitted CO_2. In their study, a capture system based on amines is implemented in conventional plants. Nevertheless, to the best of the authors' knowledge, there is still no systematic and holistic assessment of the Power-to-Methane-to-Power pathway that integrates the process with existing plants, avoids the use of fossil natural gas, considers the different available technological alternatives, and evaluates them from both technical and economic perspectives. In addition, to date, no comprehensive assessment has been carried out on the potential for retrofitting existing CCPPs to operate them as energy storage systems. Such an approach would enable the utilization of existing infrastructure to facilitate high renewable energy penetration, thereby reducing the capital investment required for large-scale implementation. Moreover, the retrofitting system evaluated in this study offers the added advantage of providing renewable synchronous generation. This capability is essential for ensuring grid stability in power systems increasingly dominated by non-synchronous and seasonal renewable sources. By repurposing existing assets, this approach directly supports current decarbonization mandates while providing the dispatchable, carbon-neutral power necessary to maintain the reliability of the electricity grid.

Therefore, this work performs a comprehensive evaluation of the Power-to-methane-to-Power cycle as a seasonal storage solution and a source of synchronous renewable generation to ensure stability in renewable-dominated grids. The power generation section is based on a combined-cycle configuration, following the layout of current natural gas power plants. Two combustion technologies are considered: conventional air combustion and oxy-fuel combustion. For CO_2 capture, three different technologies are investigated: absorption with amines (MEA), adsorption via pressure swing adsorption (PSA), and condensation, the latter being applicable only to the oxy-fuel combustion process. In the methane production section, the CO_2 captured from the power plant is combined with hydrogen produced by water electrolysis powered by renewable electricity in a methanation reactor. Accordingly, three holistic process configurations are evaluated:

a) A conventional CCPP unit coupled with MEA-based post-combustion CC.

b) A conventional CCPP unit coupled with PSA-based post-combustion CC.
c) A semi-closed oxy-combustion combined cycle unit.

A mathematical model is developed to systematically assess the three alternative configurations over scalable power plant sizes. A nonlinear optimization framework is employed to maximize key performance indicators, such as net power production. Subsequently, a techno-economic assessment is carried out to compare the three options and identify the most promising pathway in terms of efficiency and economic performance. Finally, a case study focused on the Spanish energy system is performed, in which the best-performing configuration is retrofitted to existing CCPPs of different scales to estimate the required investment costs and the levelized cost of electricity from storage. This comprehensive comparison provides new insights into the deployment of Power-to-Methane-to-Power technology as a grid-scale energy storage solution, supporting the reliability and robustness of power systems with high shares of renewable energy.

2. METHODOLOGY

The three processes analyzed in this work are: 1) Integration of CCPP with air combustion and amine absorption for carbon capture and methane production, 2) Integration of CCPP with air combustion and a PSA system for carbon capture and methane production, and 3) Integration of a CCPP with oxy-combustion and methane production. Each configuration consists of two main sections: the existing methane-based combined cycle power plant and the additional one for carbon capture and synthetic methane production. The first two processes are based on CC, which introduces a significant amount of nitrogen into the flue gas. As a result, the carbon capture system is required to separate CO_2 from the diluted exhaust stream. These two configurations differ in the type of carbon capture technology employed: one utilizes amine absorption technology, while the other employs a PSA system. The third configuration replaces air with pure oxygen (oxy-combustion). This approach results in exhaust gases composed primarily of CO_2 and water, thus eliminating the need for nitrogen separation and simplifying the CO_2 capture process.

2.1. Process Description

All processes can be divided into four subsections. 1) The combined cycle power plant where electricity is produced by burning methane. 2) The second one consists of capturing or purifying CO_2. 3) The third one corresponds to renewable hydrogen production by an electrolyzer. 4) Finally, the methanation by CO_2 with H_2. The methane generated in this section is used as feed of the first one. Thereby, the cycle can be closed. The different sections are described as follows and the flow diagram is shown in Figure 1 and Figure 2 for the CC and the OC systems respectively.

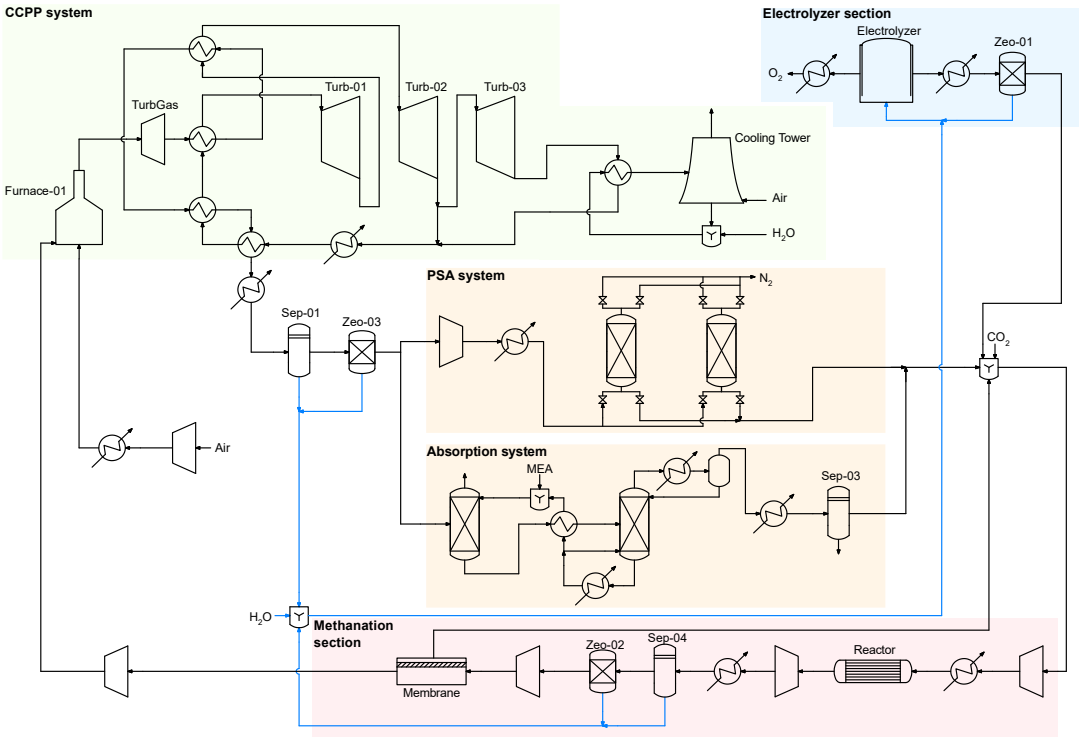

Figure 1. Flow diagram of ordinary combustion process, shown as superstructure the two alternatives for CO_2 capture systems (PSA and absorption with amines).

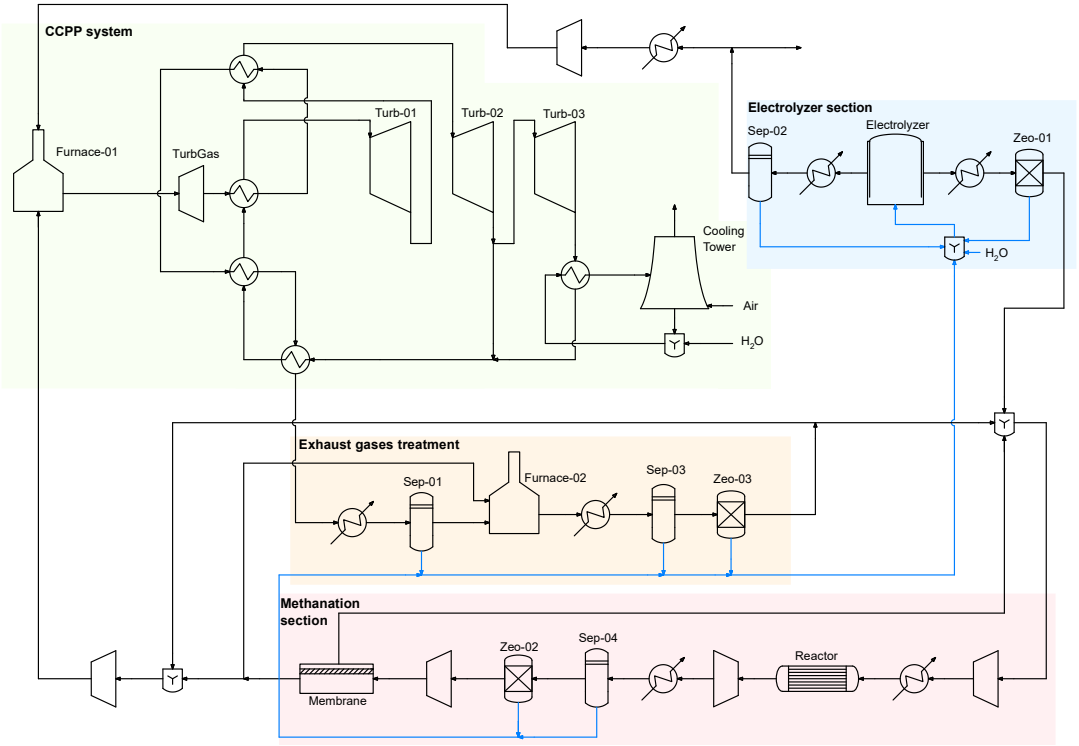

Figure 2. Flow diagram of oxy-combustion process.

2.1.1. Combined Cycle Power Plant

The combined cycle power plant is composed of two thermodynamic cycles to maximize efficiency. The first one is the Brayton cycle, which takes place in a gas turbine and the second one is the regenerative Rankine cycle with reheating, which involves a system of steam turbines (high-pressure, medium-pressure, and low-pressure turbines). The reuse of existing CCPPs is proposed, and they are also modeled to create a digital twin of the entire facility, to study the performance of the complete system. The operation of CCPP begins by introducing the feed, which has been previously conditioned, into the combustion chamber. The composition of the feed varies by process: conventional combustion uses air, whereas oxy-combustion employs pure oxygen. Nevertheless, the conditioning process is the same in all cases. The feed stream must be compressed and its temperature adjusted to the required level. The combustion chamber is modeled as adiabatic [34] where complete combustion is ensured by adding an excess of comburent. The reactions produced in this unit are presented below (Eqs. 1-3), while further details about the mass and energy balances are provided in the supplementary material.

$$CH_4 + 2O_2 \rightarrow CO_2 + 2H_2O \quad (1)$$

$$2CO + O_2 \rightarrow 2CO_2 \quad (2)$$

$$2H_2 + O_2 \rightarrow 2H_2O \quad (3)$$

Moreover, an inert spice must be introduced with the comburent to prevent the furnace temperature from exceeding the critical limit of 1600 °C and avoid material problems [35]. For conventional or CC configurations, oxygen is provided by air, which already contains a natural mixture of oxygen and nitrogen. In contrast, the oxy-combustion configuration involves recirculating part of the CO_2 exhaust back into the chamber. The gas turbine is modeled as a polytropic expansion process with an efficiency of 85% and a z parameter equal to 1.3 [36], the equation employed for modeling can be seen in the supplementary material.

The exhaust gases, after passing through the gas turbine, still contain significant thermal energy and they are utilized as a heat source for the reheater and the preheater in the regenerative Rankine cycle with reheating. In the Rankine cycle, the steam exiting the low-pressure turbine is condensed using a water refrigeration cycle with a cooling tower. The performance of the tower is modeled using Mickley's method [36] and details can be seen in the supplementary material. The increment temperature is limited to 8 - 10°C following rules of thumb to ensure proper operation. In the cooling tower, the water temperature is reduced by evaporating a fraction of the water to compensate for water losses, a make-up of water is required. To calculate it, the air humidity and water temperature in the cooling tower must be considered. In general, the CCPP section is the same for all alternative processes, but the following subsections are different for each one.

2.1.2. CO_2 Separation

The CO_2 separation section is designed to be integrated with existing CCPPs, forming an almost closed carbon loop that minimizes emissions to the atmosphere. The small amounts of CO_2 lost in the capture processes are compensated by the addition of fresh CO_2 to the system. Within a carbon capture and utilization scenario, the CO_2 makeup stream is sourced from an external capturing facility. When the methane is burned using air as the comburent the exhaust gases are composed mainly of CO_2, H_2O, a

small amount of O_2 (as it was introduced in excess) and a large amount of N_2. Nitrogen acts as an inert component and must be separated from the CO_2 to enable proper methanation. To reach the CO_2 purification, two technologies are evaluated: adsorption using PSA system and an amine-based absorption system.

The PSA columns utilize zeolite 13X as adsorbent material [37]. The operation pressure ranges from 1.1 to 3.5 bar [38], while the operating temperature varies between 25 °C and 60 °C [39]. The operating conditions of this system in the process are 1.1 bar and 30 °C. To calculate the mass of adsorbent required for the CO_2 capture process, a two-step methodology is established. First, the equilibrium capacity of the zeolite is calculated. Second, a correction factor is applied to account for the lack of ideality and the variability of the zeolite's behavior over time. The equilibrium conditions are modeled using a Langmuir solid-gas adsorption isotherm where q_m and K_L are characteristics of the material. A correlation was developed to include the effect of different temperatures on the adsorption capacity. The equations used are Eqs. (4-6).

$$q = \frac{q_m \cdot K \cdot P_{CO_2}}{1 + K \cdot P_{CO_2}} \tag{4}$$

$$q_m = -3.15551 \cdot 10^{-2}\, T(°C) + 5.02915 \tag{5}$$

$$K_L = 1.63070 \cdot 10^{-3} T(°C)^2 - 3.68332 \cdot 10^{-1} T(°C) + 27.3737 \tag{6}$$

In systems based on zeolite 13x for CO_2 capture, the operation time (τ) must be below 20 minutes to avoid loss of CO_2. Under these conditions, according to reported data, purified CO_2 is obtained with 2% nitrogen as an impurity and the small amount of oxygen [37]. However, it should be noted that the actual operating conditions of the adsorption process deviate from ideal equilibrium, and that the adsorption capacity of the zeolite decreases over multiple cycles. For this reason, a correction factor of 65% with respect to the equilibrium capacity is applied when calculating the required mass of zeolite [39]. The zeolite mass required is determined by Eq. (7). The zeolite must be replaced every 5 years [40] and its cost is assumed to be 5 $/kg [41].

$$m_{zeolite} = \frac{1}{q \cdot 0.65} \cdot \frac{fc_{CO_2} \cdot 1000}{MW_{CO_2}} \cdot \eta_{Ads} \cdot \tau \quad (7)$$

Then, the captured CO_2 is sent to the methane production section while the non-captured components from the exhaust gases, namely N_2, H_2O, O_2 and the non-adsorbed CO_2 are released into the atmosphere.

The second carbon capture system analyzed involves chemical absorption using amines. It comprises two columns, being the first one the absorption column, where the exhaust gases from the gas turbine are brought into contact with a 20 % monoethanolamine (MEA) solution. The gases which cannot be absorbed, primality nitrogen, are released into the atmosphere. The amine solution, rich in CO_2, is heated and transferred to the second column, referred to as the stripping column. In this column, the CO_2 is desorbed from the amine solution, resulting in a stream of nearly pure CO_2. To compensate for the solution losses, the amine solution is mixed with fresh MEA solution and recirculated to the absorption column. This process allows for CO_2 capture efficiencies ranging from 90% to 98% [42,43] thus an efficiency of 95% is selected. The absorption column typically operates at temperatures between 40 and 60 °C and a pressure of 100 kPa [43] while the stripping column operates at temperatures around 100 °C and pressure ranging from 200 kPa to 1500 kPa [42–44]. The temperature operation of the absorption column is 25 °C in this process, and in the stripping column is 93 °C and 2.7 bar

In contrast, the exhaust flue gases of OC are only composed of CO_2, H_2O and O_2. In this case the CO_2 must be also purified. Water is easily removed by condensation, and the elimination of the oxygen is done by sending the gases to a second combustion chamber where extra methane is added to ensure the complete remotion of oxygen. The chamber combustion temperature is limited thanks to the large amount of CO_2 there is in the inlet steam. After this step, the humidity steam is reduced by condensation to reach a better operation of the production of methane.

2.1.3. Renewable hydrogen production

For the three alternative processes, hydrogen is produced through water electrolysis. Renewable energy sources, such as wind or solar, are considered to enable the production of green hydrogen. The water required for the process is supplied by internal drying operations within the system, significantly reducing the reliance on external water sources. Nowadays, several types of electrolyzers are available: Proton

Exchange Membrane (PEM), Anion Exchange Membrane (AEM), Alkaline and Solid Oxide Ceramic (SOEC). Among them, PEM technology is selected due to the high purity of the gases produced, its advanced commercial maturity and its short start-up time [45]. PEM electrolyzers operate at temperatures up to 80 °C [46]. At this temperature their efficiency improves due to the thermodynamics enhancement [47]. Their operating pressure ranges from ambient pressure to 6 bar [48].

The electrolyzer splits water into hydrogen and oxygen, as shown in Eq. (8) generating two gaseous streams: one primarily composed of hydrogen and the other of oxygen. Both streams are subjected to a drying process to remove the residual water. The hydrogen stream is mixed with the previously purified CO_2, while the intended use of the oxygen depends on the analyzed process. The oxygen obtained in the conventional combustion process can be sold. However, the oxygen obtained in the OC process is used as a comburent in this process, eliminating the need for external oxygen supply and achieving complete integration within the process.

$$2H_2O \rightarrow 2H_2 + O_2 \quad (8)$$

2.1.4. Methane Production

The CO_2 stream, the hydrogen stream and the recirculation stream are mixed and compressed to reach the methanation reactor conditions. The methanation reactor is an isothermal multitubular fixed bed reactor with thermal control (using water as cooling agent) and a nickel-based catalysis [49]. Methane production is governed by the equations (8-11). The reactor behavior is modeled using equilibrium conditions. The typical temperature range is between 250 and 400 °C and the pressure is up to 20 bar [50].

$$CO + 3H_2 \rightleftarrows CH_4 + H_2O \quad (9)$$

$$CO_2 + H_2 \rightleftarrows CO + H_2O \quad (10)$$

$$CO_2 + 4H_2 \rightleftarrows CH_4 + 2H_2O \quad (11)$$

The feed ratio must be at least 3 as shown at Eq. (12) to avoid carbon deposition:

$$\frac{n_{H_2} + n_{CO_2}}{n_{CO} + n_{CO_2}} \geq 3 \quad (12)$$

The outlet reactor stream is expanded in a gas turbine and cooled to condense and remove water. Then, it passes through a molecular sieve of zeolites for further drying, assuming a removal efficiency of 99.97% [51]. Since the stream contains hydrogen, it is recovered by membrane separation and recycled to the methane production unit. The membrane is a polymer hollow fiber membrane and can operate at a maximum temperature of 100 °C and a pressure difference of 100 bar [52]. The hydrogen purity can reach 98.2 - 99.9% [53,54], so an average purity value of 99.0% is considered. Finally, the purified methane is sent to the CCPP combustion chamber, closing the cycle. The outlet reactor stream is expanded through a gas turbine and cooled to condense and remove water.

2.2. Optimization procedure and Techno-economic analysis

The processes are modeled using mass and energy balances, thermodynamic equilibria, experimental data and rules of thumb and they are optimized to maximize the electricity available for sale and minimize the energy consumption derived of the process. For this purpose, an NLP is formulated and solved for each of the three cases. The objective function, see Eq. (13), seeks to maximize the net power generated in the CCPP and it has been used for the optimization for every alternative process. Since each proposed process is analyzed as a separate nonlinear programming (NLP) problem, with no technology selection involved, the use of an objective function that maximizes net power output is considered appropriate. In this type of system, incoming and outgoing power flows are the key drivers of performance and have a strong influence on the cost of electricity produced from storage. The system has been modeled using an equation-based approach using GAMS and a multi start optimization with CONOPT 3.0 as the preference solver.

$$Obj = Max\ (W_{generated} - W_{consumed}) \quad (13)$$

A detailed technoeconomic analysis is performed to evaluate the processes optimized. The capital cost of each item of equipment is calculated based on the optimization results using cost correlations for the different units, in which the cost is expressed as a function of a characteristic variable, such as power for turbines or heat-transfer area for heat exchangers. For some units, a maximum feasible size is assumed;

therefore, if this limit is exceeded, multiple parallel units are required. This design choice is reflected in the corresponding capital cost calculations [55]. The investment cost is estimated from the unit costs using the factorial method [56].

The cost of electricity, following a formulation analogous to the levelized cost of storage (LCOS), is calculated as the sum of the different cost contributions from both the methanation section and the combined cycle with carbon capture. The material and utility consumption rates of the facility are determined based on the results of the process optimization. Electricity demand is assumed to be supplied from renewable sources, with an average price derived from onshore wind and solar PV of 0.041 $/kWh [57]. A cost of 0.82 $/kg or the fresh CO_2 needed to make up for losses in the capture processes is considered [58]. Additional revenues are obtained from the sale of oxygen as a by-product, with an assumed price of 0.14 $/kg [59]. Other components costs, including maintenance, labor and administration, are computed using factors from literature [56]. Annual capital expenditures are calculated considering an interest rate of 10% with 25 years as plant life.

2.3. Case of study

Different real Spanish CCPP capacities have been employed to develop a scale up study. The Spanish CCPPs can be categorized into three distinct electricity production capacity: 400 MW, 800 MW, and 1200 MW, with small deviation. Each group of a CCPP typically has a capacity of 400 MW, which means that the different types of power plants usually comprise 1, 2, or 3 groups, respectively, although there are also groups with other capacities. A summary of the power and number of groups in peninsular Spain is shown in Table 1 and a more complete table is collected in the supplementary material.

Table 1. Number of CCPP Spanish groups and their power

Groups of CCPP	Power (MW)
1	285
1	380
41	400
2	415
4	425
2	430

2	436.5
1	800
2	825
1	870

3. RESULTS

The results section is divided into 4 subsections: process details, economical results and comparisons with other chemical energy storage systems.

3.1. Process operating variables

The operating variables of the process are categorized into two groups. First, the variables related to the electrical energy section, corresponding to the combined cycle power plant are analyzed, followed by the variables of the methane production section. In Table 2, the main process variables of the combined cycle power plant are shown. The base case considers a production capacity of 400 MW. A typical CCPP usually achieves an efficiency ranging between 55 and 63% [60]. Processes based on CC fall within this range, whereas the efficiency of the OC process does not reach the lowest bound. It is important to note that the carbon capture section is not included in the efficiency presented here, as only the CCPP section is considered. This efficiency is calculated using equation 14 as the ratio between the electricity generated by the CCPP system and the energy contained in methane based on its calorific value [61].

$$\eta_{CCPP} = \frac{Total\ Power\ Generated}{Fuel_{CH_4} \cdot LHV_{CH_4}} \cdot 100 \quad (14)$$

The process variables present very similar values for configurations based on CC, as the only difference between them is the type of carbon capture technology applied. In contrast, OC configuration shows some differences. Specifically, its gas turbine generates less electrical power compared to those in the conventional configuration processes. However, this is compensated for higher electricity production from the steam turbine. To achieve this increased output, the inlet pressure of the first stream turbine is set higher than in the conventional cases.

This different behavior can be explained because the composition of combustion chamber output gases is different in both cases. As the model used for computing the energy generated in the gas turbine

(polytropic expansion) depends on the molecular weight of the gases, the energy produced is reduced in the OC case as CO_2 is the main compound and it has a higher molecular weight than nitrogen (the main compound in the CC cases).

In all cases, the gas turbine operates at its highest condition to reach a larger electrical power. The typical ranges of operation are 1600 °C and 40 bar due to material limitations. Finally, the efficiency of the combined cycle power plant is calculated, the better efficiencies are reached using CC processes.

Table 2. Technical variables of combined cycle power plant section for every approach evaluated.

Variable		**Air Combust. Absorption**	**Air Combust. PSA**	**Oxy-combustion**
Net Power	Capacity (MW)	400.00	400.00	400.00
Inlet Flow	Fuel (methane) (kg/s)	12.20	12.10	16.48
	Air or pure oxygen (kg/s)	368.25	362.68	70.61
Gas turbine	Combustion T (°C)	1600.00	1600.00	1533.47
	Inlet P (bar)	40.00	40.00	40.00
	Power Generated (MW)	328.17	327.89	263.88
Stream turbines	P high (bar)	95.00	95.00	125.00
	P medium (bar)	11.00	11.00	11.00
	P low (bar)	6.31	6.46	5.00
	T high (°C)	657.55	657.55	705.97
	T medium (°C)	552.63	552.63	552.63
	T low (°C)	457.46	460.32	429.16
	Power Generated (MW)	71.83	72.11	136.12
Efficiency	η_{CCPP} (%)	65.57	66.12	48.54

Table 3 presents the main process variables for the hydrogen and methane production sections. The oxygen used as the oxidizing agent in the OC process also originates from the electrolyzer, as it is generated simultaneously with hydrogen. Furthermore, no additional oxygen supply is required, since the amount produced is sufficient to meet the process demands. In general, the electrolyzer is the larger energy consumer, but the energy consumption is especially higher for the OC case. The reason is that in the CCPP section, that process requires the largest amount of methane to reach the same electricity production. The large difference among the power consumption caused mainly by the electrolyzer which does not allow the OC process to achieve better results. In Table 3 the yield of the hydrogen and methane production section are also presented. To determine it, equation 15 is employed to determine the energy efficiency of the Power-to-X section including carbon capture. This efficiency is based on the ratio

between the energy contained in the methane produced (as a function of its calorific value) and the energy required for the processes necessary for its production (water electrolysis, carbon capture, and methanation) [62].

$$\eta_{H_2 and\ CH_4 prod.} = \frac{Fuel_{CH_4} \cdot LHV_{CH_4}}{W_{electr} + W_{Meth} + W_{Capture}} \cdot 100 \quad (15)$$

Finally, the overall efficiency of the Power-to-methane-to-Power process is calculated by considering the ratio between the final electricity generated and the energy, mainly electrical but also thermal, introduced into the complete cycle as shown in equation 16.

$$\eta_{global} = \frac{Tot.\,Power\ Gen.}{W_{electricity} + W_{heat}} \cdot 100 \quad (16)$$

Table 3. Technical variables of hydrogen and methane production section.

Variable		**Air Combust. Absorption**	**Air Combust. PSA**	**Oxy-combustion**
Electrolyzer	Power consumption (MW)	1269.60	1264.70	1804.30
	Temperature operation (ºC)	80.00	80.00	80.00
	Pressure operation (bar)	15.00	15.00	15.00
	Hydrogen production (kg/s)	6.10	6.08	8.67
Methane Production	Temperature of operation (ºC)	310.00	310.00	310.00
	Pressure of operation (bar)	20.00	20.00	20.00
	Reactor conversion (%)	87.27	88.02	87.36
	Methane generated (kg/s)	12.15	12.11	17.27
	Fresh CO_2 (kg/s)	1.67	1.12	0.00
Efficiency H_2 and CH_4 production	$\eta_{H_2 and\ CH_4 prod.}$ (%)	24.38	23.64	22.39
Global Efficiency	η_{global} (%)	21.65	25.93	18.24

3.2. Economic results

In this section, the results of the economic analysis are presented, including the influence of economies of scale, the distribution of investment across the different process sections, and the effect of reusing the existing CCPP. The impact of power plant size on electricity production cost is illustrated in Figure 3, which shows the cost evolution profile for CCPP ranging from 100 to 1000 MW. As expected, electricity production cost decreases with increasing plant size due to economies of scale. An additional factor is the

role of oxygen sales: when oxygen is generated as a byproduct during the electrolysis process and is assumed to be completely sold (provided the market can absorb it), production costs are further reduced.

Among the processes analyzed, the most profitable configurations are the CC with absorption and the CC with a PSA system for carbon capture, with costs ranging between 450-550 $/MWh, when the oxygen is fully sold. This is followed by the CC process with PSA systems and the CC with absorption, both without oxygen sales (640-740 $/MWh) and finally, the OC process, with costs between 700-750 $/MWh.

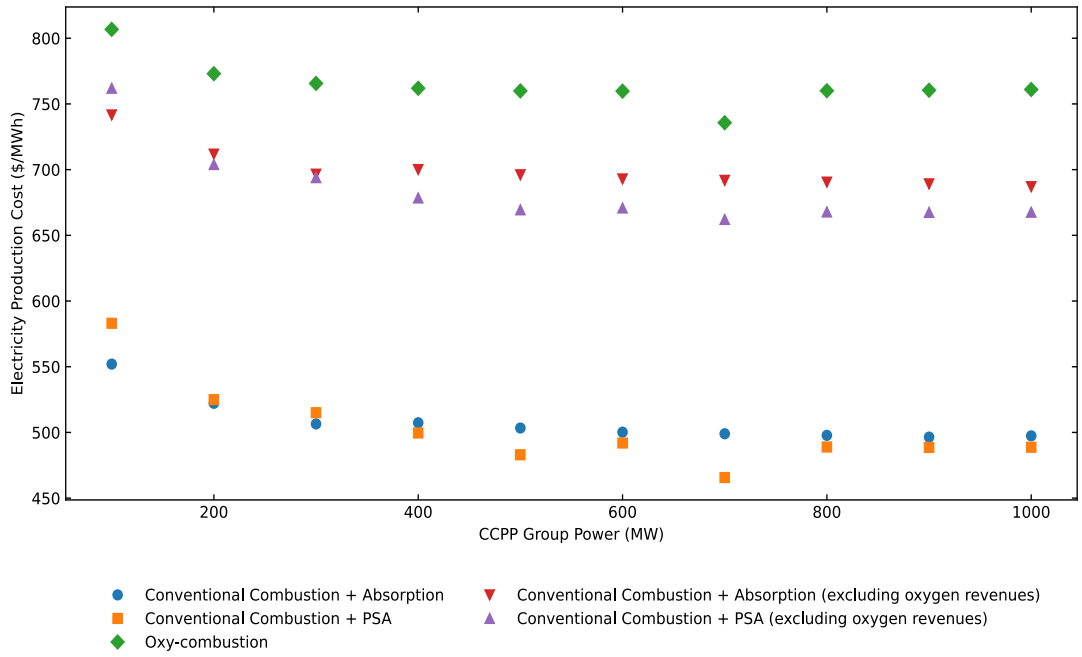

Figure 3. Comparison of electricity cost obtained with the different alternatives processes when the oxygen produced in the electrolyzer is sold as a by-product.

The large cost differences observed are mainly due to oxygen utilization. In the OC process, the oxygen produced during electrolysis is completely consumed in methane combustion, eliminating potential revenues from its sales. In contrast, CC processes assume that all byproduct oxygen is sold, providing an additional income stream that helps offset electricity production costs. Given the uncertainty of consistently selling all the oxygen produced, two extreme scenarios are considered: one in which oxygen is fully sold and another in which none is sold. These cases provide a framework for assessing the sensitivity of the overall economics of the processes to oxygen market conditions.

To further explore the economic implications, an analysis of investment distribution by process section is conducted using a 400 MW CCPP group as a case study, as this group size is the most representative among Spanish CCPP groups. The process sections are described in detail in section *2.1 Process Description,* while the corresponding results are collected in Figure 4.

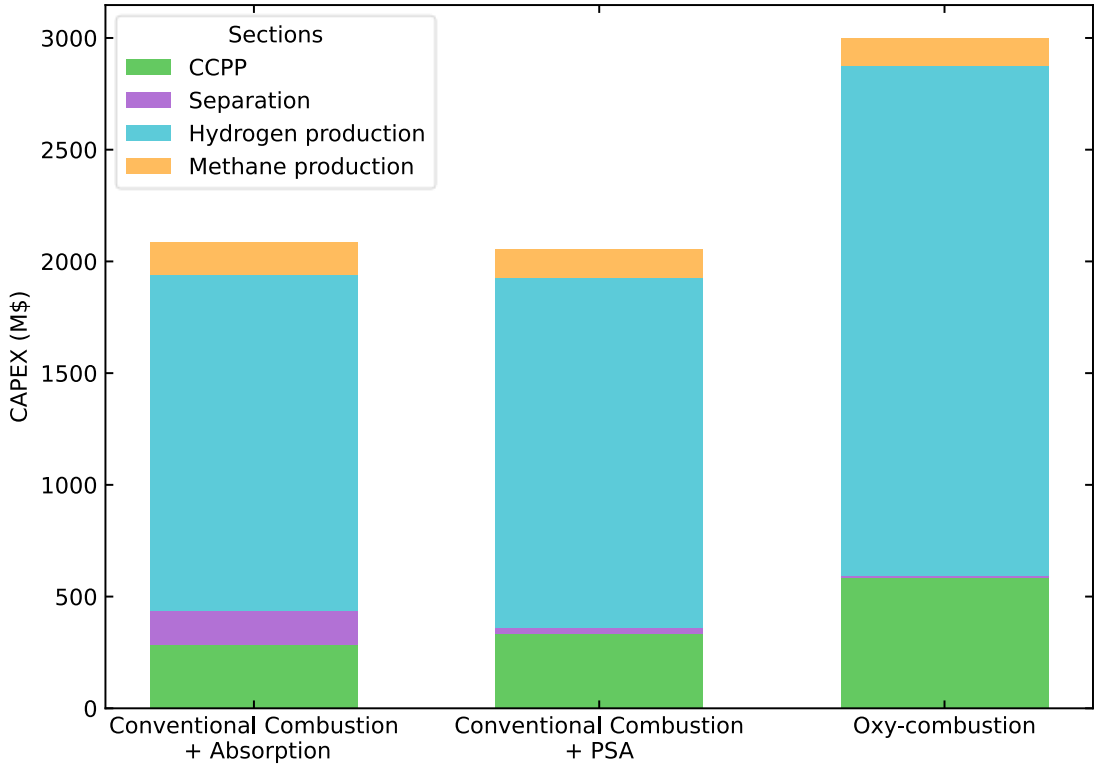

Figure 4. Breakdown of CAPEX by process section for each configuration evaluated.

The results indicate that the highest investment is associated with the hydrogen production section, basically due to the high cost of the electrolyzer, which constitutes the critical factor limiting the reduction of the overall process investment. The oxy-combustion-based configuration requires higher hydrogen production, leading to larger electrolyzer capacities and consequently larger capital investment in the electrolysis unit. This requirement significantly influences the overall investment cost of the system. However, significant cost reduction and efficiency improvements in electrolyzers are expected in the coming years, with projected capital costs decreasing from the current range of 448-1249 $/kW [63]. The separation section requires higher investment when more complex equipment is employed: absorption systems demand greater costs than PSA systems, and PSA systems are more expensive than the separation systems in oxy-combustion process. Finally, the CCPP section needs higher investment under the oxy-combustion configuration, as larger equipment is needed to achieve the same power output.

Once the process proposed has been analyzed, it is compared with other electricity generation systems. First, the system is benchmarked against direct electricity generation technologies, including current natural gas combined-cycle power plants. Second, the proposed process is compared with alternative energy storage technologies. As shown previously, among the configurations analyzed, those based on CC exhibit the most favorable cost performance, with electricity production costs ranging between 450 and 500 $/MW. For comparison, the current estimate of the Levelized Cost of Electricity (LCOE) for natural gas combined cycle power plants ranges from 12.71 to 21.10 $/MWh, while gas turbine power plants for a short-term flexible operation show LCOE values between 17.95 and 38.00 $/MWh. Projections for 2045 indicate an increase in the LCOE for combined cycle gas turbine plants, with expected values ranging from 21.68 to 47.22 $/MWh [64]. Compared to other renewable generation technologies, typical electricity costs are around 34 $/MWh for onshore wind, 43 $/MWh for solar photovoltaics, 79 $/MWh for offshore wind, and 92 $/MWh for concentrated solar power [65]. However, a direct comparison between the Power-to-Methane-to-Power system and these generation technologies is neither fully fair nor particularly meaningful. The proposed technology is an energy storage system, in which electricity that has already been produced (ideally from renewable sources) is stored and later dispatched according to the needs of the electricity system. By definition, any storage technology entails additional conversion steps and losses and is therefore inherently more expensive than direct electricity generation. For this reason, the results obtained in this work are compared below with those of other energy storage technologies. Furthermore, when considering current natural gas combined-cycle power plants, it should be noted that these facilities are increasingly affected by CO_2 emission prices. The impact of carbon pricing on generation costs is expected to continue to grow, as CO_2 prices have risen steadily in recent years, thereby putting the long-term economic viability of such plants into question. In addition, these facilities are exposed to significant volatility in natural gas prices, which directly translates into variability in electricity generation costs.

The most appropriate comparison is with other energy storage technologies, particularly those aimed at seasonal storage. For example, Schmidt et al. [66] conducted an analysis of storage costs for different applications with a 2050 time horizon. For seasonal storage, they identified four technologies as feasible options: pumped hydro, compressed air energy storage, vanadium redox flow batteries, and hydrogen.

For this application, hydrogen and its derivatives emerge as optimal and reliable solutions. Moreover, for seasonal time scales, the storage costs of alternative systems are relatively high. For instance, pumped hydro exhibits costs of around 3500 $/MWh, compressed air around 3000 $/MWh, and vanadium redox flow batteries around 20000 $/MWh, although significant cost reductions are expected in the future. These figures illustrate how chemical energy storage systems can be competitive for long-duration applications, even though their round-trip efficiency may appear lower than that of other technologies. Emrani et al. [67] carried out a comprehensive review of several parameters related to energy storage systems; however, their analysis does not differentiate between the various applications for which storage technologies are required. Among the indicators considered, the levelized cost of storage (LCOS) is selected as a key metric for comparing different technologies. Mechanical energy storage systems include technologies such as pumped hydro storage (PHS), with LCOS values ranging from 70 to 250 $/MWh. Compressed air energy storage (CAES) shows LCOS values of 60–240 $/MWh, while flywheel energy storage (FWES) exhibits higher costs, with LCOS values around 410 $/MWh. Other studies have also evaluated chemical energy carriers such as hydrogen, ammonia, or methanol as storage options. For example, a 400 MW methanol-based plant has been reported to have costs in the range of 150–890 $/MWh [68]. Hydrogen storage systems present lower costs, estimated at 450–590 $/MWh [67], mainly due to their lower equipment requirements compared to the previous options.

While mechanical storage systems generally offer more competitive LCOS values, they can present other limitations. These systems typically have lower energy density, limited scalability, and must be located in very specific geographic conditions, especially in the case of pumped hydro storage. In contrast, chemical storage systems offer a significant advantage in terms of geographical adaptability, scalability, and suitability for long-term or seasonal storage. Among chemical systems, methane, methanol and ammonia present a clear advantage for storage if they are compared with hydrogen storage systems technologies. The main advantage of the configuration proposed in this work is the use of methane as a chemical energy storage system lies in the existing infrastructure for converting methane into electricity. In contrast, the use of methanol or ammonia would require the construction of new plants for this purpose. By integrating carbon capture, hydrogen production, and methane synthesis directly into the CCPPs, the need for new facilities is avoided, while simultaneously extending the useful life of current plants.

Table 4. Economic indicators (CAPEX, OPEX, Total Production Cost and Production Cost per unit) for the alternative process configurations considering retrofitting of existing CCPPs and construction of new plants.

		CAPEX (M$)	OPEX (M$/year)	Total production cost (M$/year)	Production cost ($/MWh)
Considering the use of current CCPP	**CC + Amine**	6910.03	840.31	827.43	444.87
	CC + PSA system	6704.33	831.23	822.80	427.89
	Oxy-combustion	9410.72	1164.97	1635.53	664.57
Considering the construction of a CCPP	**CC + Amine**	8015.38	901.25	943.63	507.35
	CC + PSA system	8015.56	903.52	960.64	499.57
	Oxy-combustion	11689.41	1290.59	1875.08	761.91

Another relevant aspect to analyze is the economic impact of constructing a new CCPP for the proposed system or making use of the existing CCPP infrastructure. Table 4 presents the results for both scenarios across the three configurations evaluated (CC with amine adsorption, CC with a PSA system and oxy-combustion) considering a reference plant size of 400 MW. The analysis indicates that reusing current installations leads to a cost reduction of approximately 10% compared to the construction of new plants.

This highlights the significant investment required to implement the proposed energy storage system, as well as demonstrating the cost reduction advantage achieved when it is integrated with the existing infrastructure. Moreover, although not considered in the analysis, suitable storage infrastructure already

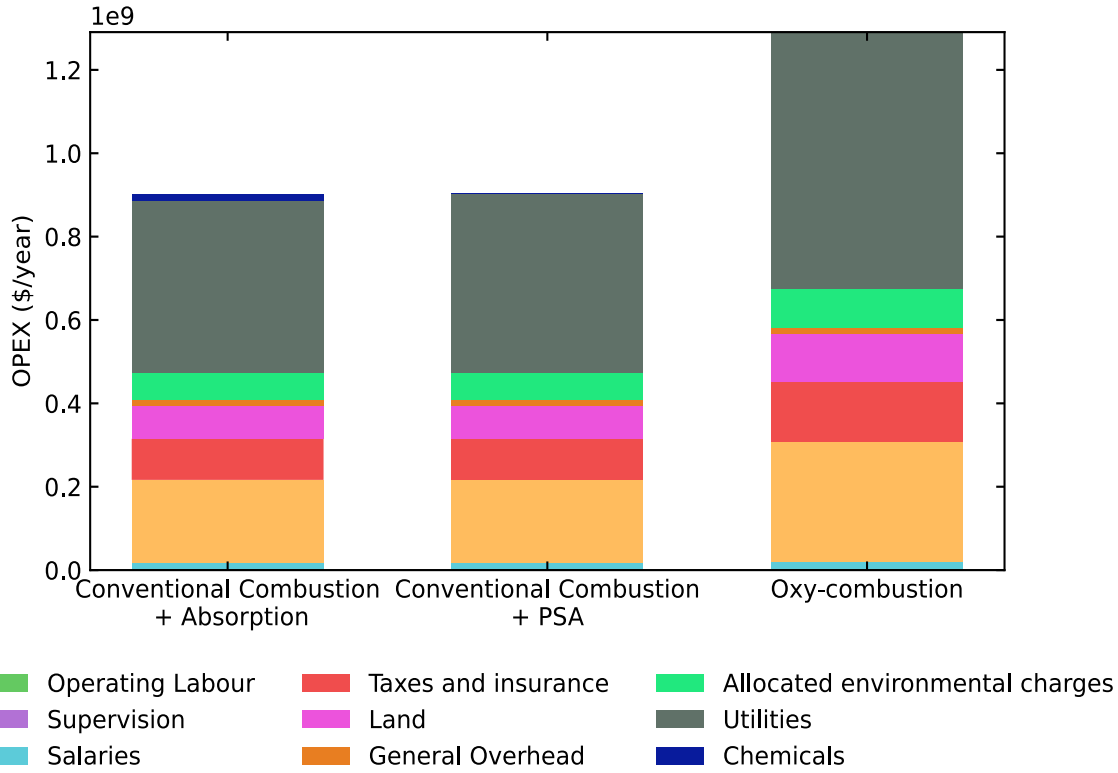

Figure 5. Breakdown of CAPEX by process section for each configuration evaluated.

exists, as the same facility currently used for fossil natural gas can be employed for synthetic methane storage. Nevertheless, the oxy-combustion configuration remains the most expensive option, even when assuming the use of an existing CCPP for this process and the construction of a new one for the other configurations.

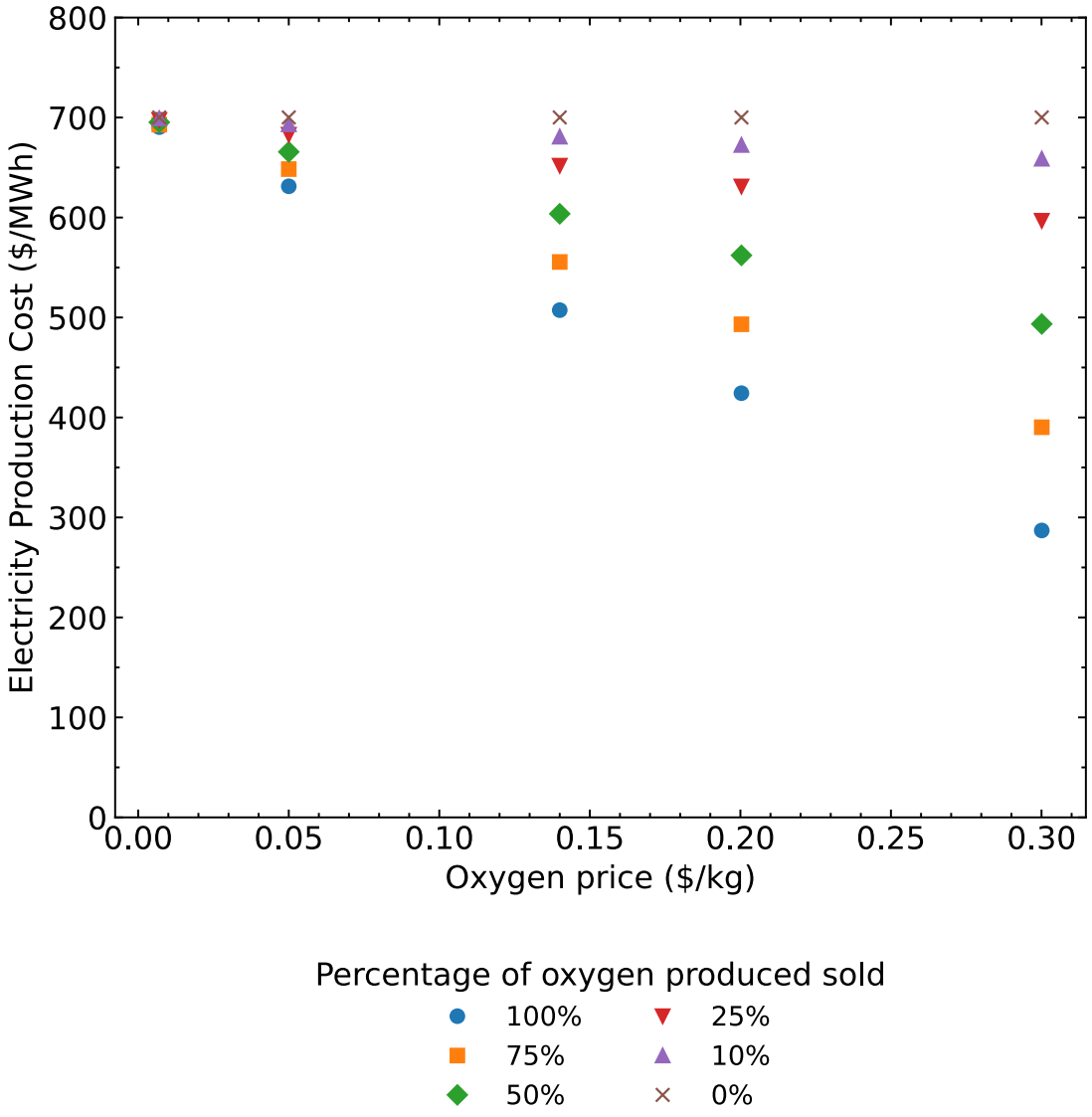

Figure 6. Sensitivity analysis of oxygen sales for an electricity production of 400 MW. The effect of variations in oxygen prices and the percentage of oxygen sold on the cost of electricity production is shown.

3.3. Sensitivity Analysis

As discussed in the previous section, several factors significantly influence the economic performance of the Power-to-Methane-to-Power process. In particular, this section presents a sensitivity analysis focusing on two key parameters: the potential revenue from the sale of oxygen generated during electrolysis (in

configurations employing conventional air combustion) and the price of renewable electricity supplied to the electrolysis unit.

First, the impact of oxygen commercialization is analyzed. In the previous section, the analysis was conducted assuming an oxygen sale price of 0.14 $/kg and considering two extreme scenarios: complete sale of the O_2 produced and no possibility of commercialization. In the present sensitivity study, a broader range of oxygen prices (0–0.30 $/kg) is evaluated, together with different percentages of the total O_2 production from electrolysis that can be sold. The resulting impact on the cost of electricity from storage is presented in Figure 6.

The results clearly demonstrate the significant impact of oxygen commercialization on the cost of electricity from the storage system. Differences of up to 57% are observed between the scenarios analyzed, highlighting the strong dependence of economic performance on this parameter. This sensitivity analysis reflects realistic operational conditions, as the highly volatile nature of the oxygen market makes it impossible to guarantee that the entire O_2 production can be sold to end users. It should also be considered that a large-scale deployment of renewable hydrogen projects could lead to an oversupply of oxygen relative to existing market demand, thereby reducing the economic value of this by-product. Consequently, exploring potential integrations of the proposed process with other chemical or energy-intensive industries could be of particular interest, enabling internal utilization of the produced O_2 and ensuring more complete valorization of all output streams.

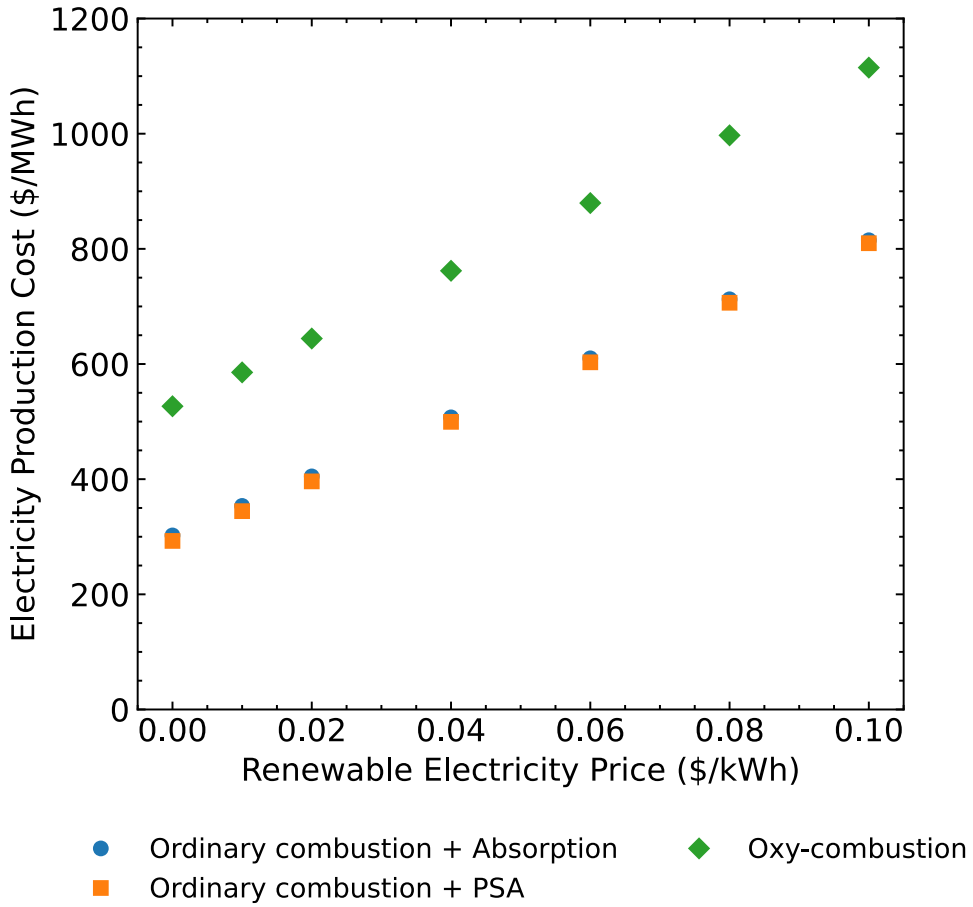

Figure 7. Sensitivity analysis of renewable electricity price. The effect of variation in renewable electricity price on the electricity production cost is shown.

Secondly, the impact of the electricity price supplied to the electrolysis unit is analyzed, with particular emphasis on its influence on the final cost of electricity generated from storage. The primary objective of the Power-to-Methane-to-Power process is to enable the integration of renewable electricity sources through large-scale energy storage. In the base case, an electricity cost of 0.041 $/kWh is assumed, representing an approximate average across different renewable generation technologies. According to the International Renewable Energy Agency [65], the levelized cost of renewable electricity is approximately 0.034 $/kWh for onshore wind, 0.043 $/kWh for solar photovoltaics, 0.079 $/kWh for offshore wind, 0.092 $/kWh for concentrated solar power, 0.057 $/kWh for hydropower, and 0.087 $/kWh for bioenergy. Based on these values, a sensitivity analysis is performed considering electricity prices in the range of 0–0.1 $/kWh, thereby covering a bro4ad spectrum of potential operating conditions for the proposed system. The lower bound is set to 0 $/kWh to account for periods of very high renewable

generation, during which wholesale market prices may reach zero or even negative values due to excess supply from non-dispatchable sources. Under such conditions, energy storage (particularly seasonal storage) becomes especially relevant. The upper bound reflects the observed cost range of the various renewable technologies. The results of this analysis are presented in Figure 7 for a nominal production capacity of 400 MW.

The results highlight the critical influence of the cost of electricity supplied to the electrolysis unit on the final cost of electricity generated from storage. In particular, when the cost of input electricity is sufficiently low, the resulting storage-based electricity cost can become highly competitive for seasonal applications, reaching values on the order of 300 $/MWh. Under such conditions, seasonal storage can effectively prevent the curtailment of a significant share of renewable generation while enhancing overall system robustness and reliability.

3.4. Comparison among different production capacities.

CCPPs offer greater operational flexibility compared to other electricity generation systems, as they can be started and put into operation within a few hours. This capability makes them particularly suitable for balancing fluctuations in electricity demand, especially during periods of insufficient renewable energy production. Consequently, production capacity has a considerable influence on the economic outcomes. To illustrate this effect, a 400 MW CCPP is used as a reference case to evaluate how both the total cost of production (TCOP) and the electricity production cost vary with changes in production capacity across the different processes. Since turbine efficiency decreases under partial load conditions, it is necessary to incorporate a load-dependent efficiency correction which is calculated using the following equation:

$$\eta_{real} = \eta_s v \tag{17}$$

Where v is the adjustment factor to introduce the load influence in the turbine efficiency [69]:

$$v = 1 - (0.191 - 0.409 \cdot load + 0.218 \cdot load^2) \tag{18}$$

The evolution of the total annual cost assuming the oxygen generated is sold is shown in Figure 8 a), while the corresponding case without oxygen sales is presented in Figure 8 c). The comparison reveals that

revenues from oxygen sales significantly contribute to reducing the total production cost, as evidenced by the differences between Figure 8 b) and Figure 8 d). In absence of O_2 credits, the cost curves for CC processes closely follow those of OC process. With respect to electricity production cost the impact of oxygen sales is less pronounced. However, when oxygen is not sold, the electricity production cost for the CC process becomes more comparable to that of OC process, Figure 5 d).

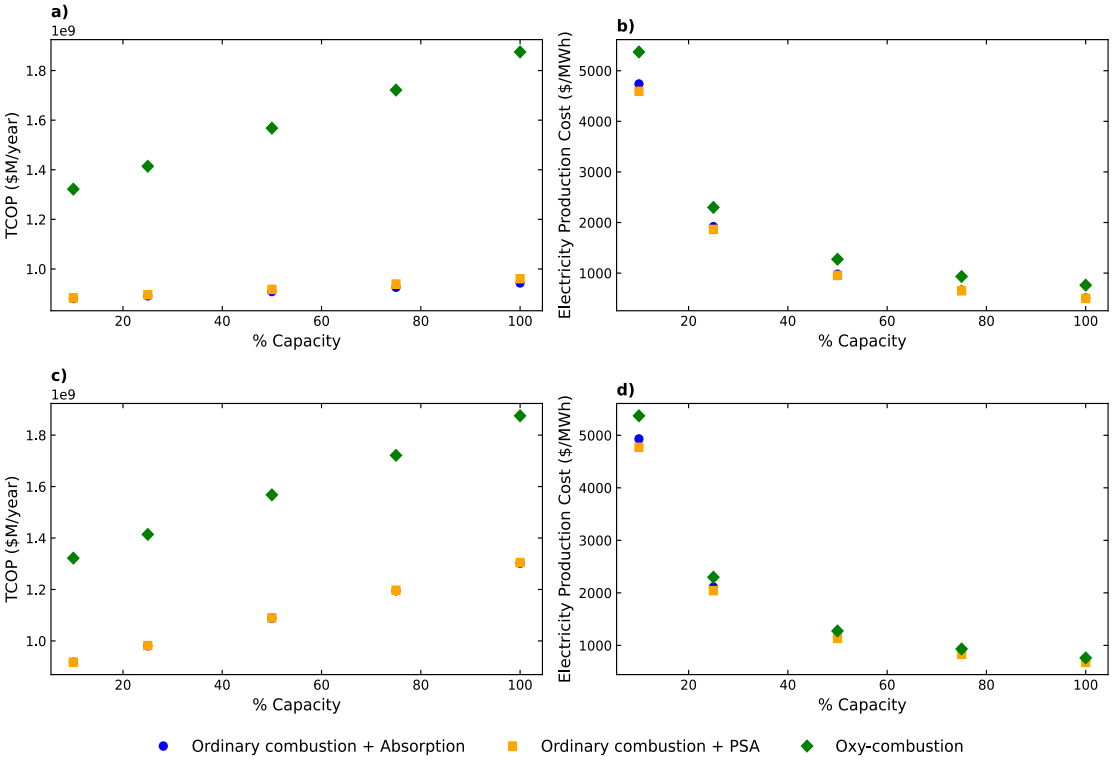

Figure 8. a) Comparison of the total annual cost of electricity production for each alternative process for different production capacities when the oxygen produced in the electrolyzer is completely sold as a by-product. b) Evolution of the cost of electricity production for each alternative process at different plant capacities when the oxygen produced in the electrolyzer is completely sold as a by-product. c) Comparison of the total annual cost of electricity production for each alternative process for different production capacities when the oxygen produced in the electrolyzer is not sold as a by-product. d) Evolution of the cost of electricity production for each alternative process at different plant capacities when the oxygen produced in the electrolyzer is not sold as a by-product.

The reduction in turbine efficiency is more evident when the plant operates below 50% capacity. As shown in Figure 8b) and 8d), this efficiency drop leads to a significant increase in electricity production cost. Therefore, maintaining an operating capacity above 50% is necessary to avoid excessively high electricity production costs. Although the total cost of production decreases with reduced plant capacity, mainly due to lower utility requirements, the decline in efficiency results in higher specific electricity production cost at lower loads.

3.5. Case study: Spanish CCPP.

In this section, Spanish CCPPs are used as a case study to evaluate their integration with methane as energy storage system. In this approach, investment costs are reduced thanks to the existing CCPPs and the natural gas storage infrastructure, which can also be utilized for synthetic methane. Figure 9 presents

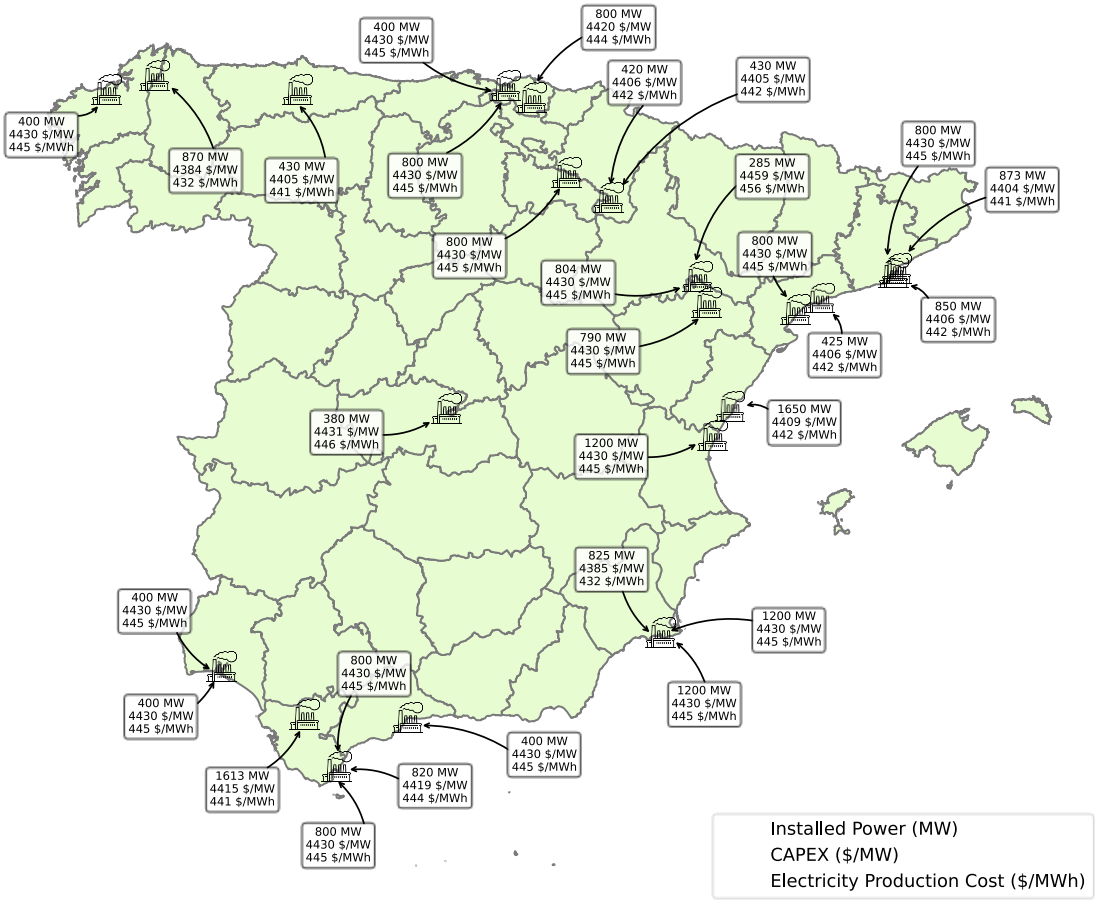

Figure 9. Maps of Spanish natural gas CCPPs, with each plant located in its respective province. Each square represents a plant, and the data inside follow the legend order.

the 30 CCPPs located in peninsular Spain. Each square in the figure represents one CCPP, which may consist of 1, 2 or 3 groups, although the data presented corresponds to the overall aggregated results. For simplicity, plants are positioned within their respective provinces rather than their exact geographic locations. Each square displays 3 indicators: the installed power capacity, the CAPEX associated with the proposed system (excluding the CCPP investment), and the resulting electricity production cost. A significant reduction in investment costs can be observed, resulting in a corresponding decrease in electricity production costs. The required investment ranges from 2778 to 2836 $/MW, while the electricity production cost varies from 327 to 346 $/MWh.

It may seem evident that larger plants benefit from lower electricity production costs due to economies of scale. However, most of these plants consist of 2 or 3 CCPP groups, each with an installed capacity between 400 and 800 MW. In this context, the most competitive production costs are obtained in plants that incorporate the largest CCPP groups currently operating in Spain. These groups, with capacities close to 800 MW, achieve the lowest production costs despite not requiring the lower CAPEX for the installation of the storage system. This highlights that the configuration and the groups size play a decisive role in determining economic performance.

4. CONCLUSIONS

This work presents a holistic evaluation of the Power-to-Methane-to-Power system as a grid-scale energy storage solution. The system proposed consists of two main sections: methane synthesis and electricity generation. In the power generation stage, a combined-cycle configuration coupled with a CO_2 capture process is considered. Two combustion concepts are analyzed (conventional air combustion and oxy-fuel combustion) and several capture technologies are evaluated, namely absorption, adsorption, and condensation.

The results demonstrate the technical feasibility of implementing this type of process, achieving overall energy efficiencies in the range of approximately 20–30%. Although these values are low compared to short-term, fast-response storage technologies, they are reasonable for large-scale, seasonal energy storage applications. The resulting cost of electricity from storage is estimated to lie in the range of approximately 500–700 $/MWh, with higher values observed for the oxy-fuel combustion configurations. These values are promising, particularly when compared with other technologies proposed for seasonal storage. Two key factors governing the economic performance of this system are the cost of the input renewable electricity and the potential revenue from selling the oxygen produced as a by-product.

In addition, this study explores the integration of Power-to-Methane-to-Power processes into existing natural gas combined-cycle power plants, enabling partial reuse of the current infrastructure. This approach allows the benefits of combined-cycle technology to be retained while transitioning to a renewable-based system, thereby reducing the investment costs associated with this storage option. A case study focusing on Spain, which has a large fleet of combined-cycle power plants, is presented to

estimate the required investment and the resulting electricity costs under the assumption of infrastructure reuse at the plant level. The results highlight the significant potential of this storage technology in future energy systems with high shares of renewable generation, contributing to a secure and reliable power supply that is essential for economic development. Finally, future research should address detailed comparisons with other storage technologies from both economic and environmental perspectives, as well as potential synergies with other industrial processes, to further improve the proposed concept.

ACKNOWLEDGMENTS

This work was supported by the funding received from the Ministry of Science, Innovation and Universities, PID2023-1462310B-I00.

REFERENCES

[1] European Union. Regulation (EU) 2021/1119 of the European Parliament and of the Council of 30 June 2021 establishing the framework for achieving climate neutrality and amending Regulations (EC) No 401/2009 and (EU) 2018/1999 ('European Climate Law'). 2021.

[2] European Environment Agency. Share of energy consumption from renewable sources in Europe | European Environment Agency's home page 2025. https://www.eea.europa.eu/en/analysis/indicators/share-of-energy-consumption-from (accessed September 11, 2025).

[3] European Union. Directive (EU) 2023/2413 of the European Parliament and of the Council of 18 October 2023 amending Directive (EU) 2018/2001, Regulation (EU) 2018/1999 and Directive 98/70/EC as regards the promotion of energy from renewable sources, and repealing Council Directive (EU) 2015/652. 2023.

[4] Schmietendorf K, Peinke J, Kamps O. The impact of turbulent renewable energy production on power grid stability and quality. The European Physical Journal B 2017 90:11 2017;90:1–6. https://doi.org/10.1140/EPJB/E2017-80352-8.

[5] Elalfy DA, Gouda E, Kotb MF, Bureš V, Sedhom BE. Comprehensive review of energy storage systems technologies, objectives, challenges, and future trends. Energy Strategy Reviews 2024;54:101482. https://doi.org/10.1016/J.ESR.2024.101482.

[6] Bhandari R, Adhikari N. A comprehensive review on the role of hydrogen in renewable energy systems. Int J Hydrogen Energy 2024;82:923–51. https://doi.org/10.1016/J.IJHYDENE.2024.08.004.

[7] Abdin Z, Zafaranloo A, Rafiee A, Mérida W, Lipiński W, Khalilpour KR. Hydrogen as an energy vector. Renewable and Sustainable Energy Reviews 2020;120:109620. https://doi.org/10.1016/J.RSER.2019.109620.

[8] Usman MR. Hydrogen storage methods: Review and current status. Renewable and Sustainable Energy Reviews 2022;167:112743. https://doi.org/10.1016/J.RSER.2022.112743.

[9] Gonzalez-Salazar MA, Kirsten T, Prchlik L. Review of the operational flexibility and emissions of gas- and coal-fired power plants in a future with growing renewables. Renewable and Sustainable Energy Reviews 2018;82:1497–513. https://doi.org/10.1016/j.rser.2017.05.278.

[10] Kanniche M, Gros-Bonnivard R, Jaud P, Valle-Marcos J, Amann JM, Bouallou C. Pre-combustion, post-combustion and oxy-combustion in thermal power plant for CO2 capture. Appl Therm Eng 2010;30:53–62. https://doi.org/10.1016/J.APPLTHERMALENG.2009.05.005.

[11] Jansen D, Gazzani M, Manzolini G, Dijk E Van, Carbo M. Pre-combustion CO2 capture. International Journal of Greenhouse Gas Control 2015;40:167–87. https://doi.org/10.1016/J.IJGGC.2015.05.028.

[12] Kazemi A, Moreno J, Iribarren D. Techno-economic comparison of optimized natural gas combined cycle power plants with CO2 capture. Energy 2022;255:124617. https://doi.org/10.1016/J.ENERGY.2022.124617.

[13] Kammerer S, Borho I, Jung J, Schmidt MS. Review: CO2 capturing methods of the last two decades. International Journal of Environmental Science and Technology 2023;20:8087–104. https://doi.org/10.1007/S13762-022-04680-0/FIGURES/14.

[14] Global CCS Institute. The 2024 Global Status of CCS 2024. https://doi.org/https://www.globalccsinstitute.com/resources/global-status-report/.

[15] Jiang L, Gonzalez-Diaz A, Ling-Chin J, Roskilly AP, Smallbone AJ. Post-combustion CO2 capture from a natural gas combined cycle power plant using activated carbon adsorption. Appl Energy 2019;245:1–15. https://doi.org/10.1016/J.APENERGY.2019.04.006.

[16] Xiang Y, Cai L, Guan Y, Liu W, Han Y, Liang Y. Study on the configuration of bottom cycle in natural gas combined cycle power plants integrated with oxy-fuel combustion. Appl Energy 2018;212:465–77. https://doi.org/10.1016/J.APENERGY.2017.12.049.

[17] Bolland O, Mathieu P. Comparison of two CO2 removal options in combined cycle power plants. Energy Convers Manag 1998;39:1653–63. https://doi.org/https://doi.org/10.1016/S0196-8904(98)00078-8.

[18] Michael K, Golab A, Shulakova V, Ennis-King J, Allinson G, Sharma S, et al. Geological storage of CO2 in saline aquifers—A review of the experience from existing storage operations. International Journal of Greenhouse Gas Control 2010;4:659–67. https://doi.org/10.1016/J.IJGGC.2009.12.011.

[19] Anicic B, Trop P, Goricanec D. Comparison between two methods of methanol production from carbon dioxide. Energy 2014;77:279–89. https://doi.org/10.1016/J.ENERGY.2014.09.069.

[20] Martín M. Methodology for solar and wind energy chemical storage facilities design under uncertainty: Methanol production from CO2 and hydrogen. Comput Chem Eng 2016;92:43–54. https://doi.org/10.1016/J.COMPCHEMENG.2016.05.001.

[21] Devkota S, Karmacharya P, Maharjan S, Khatiwada D, Uprety B. Decarbonizing urea: Techno-economic and environmental analysis of a model hydroelectricity and carbon capture based green

urea production. Appl Energy 2024;372:123789. https://doi.org/https://doi.org/10.1016/j.apenergy.2024.123789.

[22] Pérez-Fortes M, Schöneberger JC, Boulamanti A, Harrison G, Tzimas E. Formic acid synthesis using CO2 as raw material: Techno-economic and environmental evaluation and market potential. Int J Hydrogen Energy 2016;41:16444–62. https://doi.org/10.1016/J.IJHYDENE.2016.05.199.

[23] Rumayor M, Dominguez-Ramos A, Irabien A. Formic Acid Manufacture: Carbon Dioxide Utilization Alternatives. Applied Sciences 2018, Vol 8, Page 914 2018;8:914. https://doi.org/10.3390/APP8060914.

[24] Bassano C, Deiana P, Lietti L, Visconti CG. P2G movable modular plant operation on synthetic methane production from CO2 and hydrogen from renewables sources. Fuel 2019;253:1071–9. https://doi.org/10.1016/J.FUEL.2019.05.074.

[25] Davis W, Martín M. Optimal year-round operation for methane production from CO2 and water using wind and/or solar energy. J Clean Prod 2014;80:252–61. https://doi.org/https://doi.org/10.1016/j.jclepro.2014.05.077.

[26] Skocek J, Zajac M, Ben Haha M. Carbon Capture and Utilization by mineralization of cement pastes derived from recycled concrete. Sci Rep 2020;10:5614. https://doi.org/10.1038/s41598-020-62503-z.

[27] Shi Y, Su W, Xing Y, Cui Y, Liu X, Guo W, et al. Research progress and future prospects of chemical utilization of CO2. Chemical Engineering Journal 2025;510:161579. https://doi.org/10.1016/J.CEJ.2025.161579.

[28] Romeo LM, Cavana M, Bailera M, Leone P, Peña B, Lisbona P. Non-stoichiometric methanation as strategy to overcome the limitations of green hydrogen injection into the natural gas grid. Appl Energy 2022;309:118462. https://doi.org/https://doi.org/10.1016/j.apenergy.2021.118462.

[29] Meylan FD, Moreau V, Erkman S. Material constraints related to storage of future European renewable electricity surpluses with CO2 methanation. Energy Policy 2016;94:366–76. https://doi.org/10.1016/J.ENPOL.2016.04.012.

[30] Fonder M, Counotte P, Dachet V, de Séjournet J, Ernst D. Synthetic methane for closing the carbon loop: Comparative study of three carbon sources for remote carbon-neutral fuel synthetization. Appl Energy 2024;358:122606. https://doi.org/10.1016/J.APENERGY.2023.122606.

[31] Pyo MJ, Moon SW, Kim TS. A Comparative Feasibility Study of the Use of Hydrogen Produced from Surplus Wind Power for a Gas Turbine Combined Cycle Power Plant. Energies 2021, Vol 14, Page 8342 2021;14:8342. https://doi.org/10.3390/EN14248342.

[32] Kezibri N, Bouallou C. Conceptual design and modelling of an industrial scale power to gas-oxy-combustion power plant. Int J Hydrogen Energy 2017;42:19411–9. https://doi.org/10.1016/J.IJHYDENE.2017.05.133.

[33] Prakash D, Singh O. Thermo-economic study of combined cycle power plant with carbon capture and methanation. J Clean Prod 2019;231:529–42. https://doi.org/10.1016/J.JCLEPRO.2019.05.217.

[34] León E, Martín M. Optimal production of power in a combined cycle from manure based biogas. Energy Convers Manag 2016;114:89–99. https://doi.org/10.1016/J.ENCONMAN.2016.02.002.

[35] Singh K. Advanced Materials for Land Based Gas Turbines. Transactions of the Indian Institute of Metals 2014;67:601–15. https://doi.org/10.1007/S12666-014-0398-3/FIGURES/16.

[36] Guerras LS, Martín M. On the water footprint in power production: Sustainable design of wet cooling towers. Appl Energy 2020;263:114620. https://doi.org/https://doi.org/10.1016/j.apenergy.2020.114620.

[37] Martín-Hernández E, Guerras LS, Martín M. Optimal technology selection for the biogas upgrading to biomethane. J Clean Prod 2020;267:122032. https://doi.org/https://doi.org/10.1016/j.jclepro.2020.122032.

[38] Riboldi L, Bolland O. Overview on pressure swing adsorption (PSA) as CO2 capture technology: state-of-the-art, limits and potentials. Energy Procedia 2017;114:2390–400.

[39] Hauchhum L, Mahanta P. Carbon dioxide adsorption on zeolites and activated carbon by pressure swing adsorption in a fixed bed. International Journal of Energy and Environmental Engineering 2014;5:349–56.

[40] Xiao G, Webley P, Hoadley A, Ho M, Wiley D. Low Cost Hybrid Capture Technology Development 2013.

[41] Kouchachvili L, Bardy DA, Djebbar R, Hogg LEW. Natural zeolites as host matrices for the development of low-cost and stable thermochemical energy storage materials. Journal of Porous Materials 2023;30:163–73.

[42] Olajire AA. CO2 capture and separation technologies for end-of-pipe applications–A review. Energy 2010;35:2610–28.

[43] Xue B, Yu Y, Chen J, Luo X, Wang M. A comparative study of MEA and DEA for post-combustion CO2 capture with different process configurations. Int J Coal Sci Technol 2017;4:15–24.

[44] Wang M, Lawal A, Stephenson P, Sidders J, Ramshaw C. Post-combustion CO2 capture with chemical absorption: A state-of-the-art review. Chemical Engineering Research and Design 2011;89:1609–24.

[45] Akyüz ES, Telli E, Farsak M. Hydrogen generation electrolyzers: Paving the way for sustainable energy. Int J Hydrogen Energy 2024;81:1338–62.

[46] Alkhaldi S, Aziz M, Amrite A, Prasad AK. Parametric study of PEM water electrolyzer performance. J Appl Electrochem 2024:1–17. https://doi.org/10.1007/S10800-024-02187-9/FIGURES/15.

[47] Bazarah A, Majlan EH, Husaini T, Zainoodin AM, Alshami I, Goh J, et al. Factors influencing the performance and durability of polymer electrolyte membrane water electrolyzer: A review. Int J Hydrogen Energy 2022;47:35976–89. https://doi.org/10.1016/J.IJHYDENE.2022.08.180.

[48] Debe MK, Hendricks SM, Vernstrom GD, Meyers M, Brostrom M, Stephens M, et al. Initial performance and durability of ultra-low loaded NSTF electrodes for PEM electrolyzers. J Electrochem Soc 2012;159:K165.

[49] Santamaría D, Sánchez A, Martín M. Scaling down analysis of e-methane production: Advancing towards distributed manufacturing. Renew Energy 2025;245:122792. https://doi.org/10.1016/j.renene.2025.122792.

[50] Stangeland K, Kalai D, Li H, Yu Z. CO2 Methanation: The Effect of Catalysts and Reaction Conditions. Energy Procedia 2017;105:2022–7. https://doi.org/https://doi.org/10.1016/j.egypro.2017.03.577.

[51] Davis W, Martín M. Optimal year-round operation for methane production from CO2 and water using wind energy. Energy 2014;69:497–505.

[52] UBE Corporation. H2 Separation Membrane Module. UBE Corporation 2024. https://www.ube.com/contents/en/chemical/separation/hydrogen_separation_membrane.html (accessed January 30, 2024).

[53] Meindersma GW. Membrane permeation and pressure swing adsorption (PSA) for the production of high purity hydrogen. Effective Industrial Membrane Processes: Benefits and Opportunities, Springer; 1991, p. 391–400.

[54] Ockwig NW, Nenoff TM. Membranes for Hydrogen Separation. Chem Rev 2007;107:4078–110.

[55] Sánchez A, Martín M. Scale up and scale down issues of renewable ammonia plants: Towards modular design. Sustain Prod Consum 2018;16:176–92.

[56] Sinnott R, Towler G. Chemical engineering design: SI Edition. Butterworth-Heinemann; 2019.

[57] IRENA. RENEWABLE POWER GENERATION COSTS IN 2022 2 R E N E WAB LE P OWE R G E N E R ATI O N COS TS I N 202 2. International Renewable Energy Agency 2022.

[58] Eurostat. Eurostat. Natural Gas Price Statistics 2025. https://ec.europa.eu/eurostat/databrowser/view/nrg_pc_203__custom_14012008/default/table?lang=en (accessed February 10, 2025).

[59] Yuanrong Zhou; Stephanie Searle. Cost of renewable hydrogen produced onsite at hydrogen refueling stations in Europe. 2022.

[60] IPIECA. Combined-cycle gas turbines 2022. https://www.ipieca.org/resources/energy-efficiency-compendium/combined-cycle-gas-turbines-2022 (accessed February 11, 2025).

[61] Bao J, Zhang L, Song C, Zhang N, Guo M, Zhang X. Reduction of efficiency penalty for a natural gas combined cycle power plant with post-combustion CO2 capture: Integration of liquid natural gas cold energy. Energy Convers Manag 2019;198:111852. https://doi.org/10.1016/j.enconman.2019.111852.

[62] Battaglia V, Vanoli L. Optimizing renewable energy integration in new districts: Power-to-X strategies for improved efficiency and sustainability. Energy 2024;305:132312. https://doi.org/10.1016/j.energy.2024.132312.

[63] Krishnan S, Koning V, Theodorus de Groot M, de Groot A, Mendoza PG, Junginger M, et al. Present and future cost of alkaline and PEM electrolyser stacks. Int J Hydrogen Energy 2023;48:32313–30. https://doi.org/10.1016/J.IJHYDENE.2023.05.031.

[64] Kost C, Müller P, Sepúlveda Schweiger J, Fluri V, Thomsen J. Levelized Cost of Electricity Renewable Energy Technologies. Freiburg: 2024.

[65] IRENA. Green Hydrogen Cost Reduction: Scaling up Electrolysers to Meet the 1.5^{0}C Climate Goal. International Renewable Energy Agency 2020.

[66] Schmidt O, Melchior S, Hawkes A, Staffell I. Projecting the Future Levelized Cost of Electricity Storage Technologies. Joule 2019;3:81–100. https://doi.org/10.1016/j.joule.2018.12.008.

[67] Emrani A, Berrada A. A comprehensive review on techno-economic assessment of hybrid energy storage systems integrated with renewable energy. J Energy Storage 2024;84:111010. https://doi.org/10.1016/J.EST.2024.111010.

[68] Blanco EC, Sánchez A, Martín M, Vega P. Methanol and ammonia as emerging green fuels: Evaluation of a new power generation paradigm. Renewable and Sustainable Energy Reviews 2023;175:113195. https://doi.org/10.1016/J.RSER.2023.113195.

[69] National Renewable Energy Laboratory. System Advisor Model (SAM) 2025. https://sam.nrel.gov/ (accessed June 17, 2025).